Polymer Chemistry

PAPER

View Article Online
View Journal

Check for updates

Cite this: DOI: 10.1039/c7py01690e

A photocatalyst immobilized on fibrous and porous monolithic cellulose for heterogeneous catalysis of controlled radical polymerization†

Yingying Chu,[a] Zixuan Huang,[a] Kang Liang,[b,c] Jia Guo,[d] Cyrille Boyer *[a] and Jiangtao Xu *[a]

Received 5th October 2017,
Accepted 30th October 2017

DOI: 10.1039/c7py01690e

rsc.li/polymers

Natural fibrous cellulose (cotton) and household porous cellulose (sponge) as supporting monolithic materials were employed for the immobilization of a photoredox catalyst to prepare unique heterogeneous catalyst composites, which were able to effectively regulate controlled radical polymerization of diverse monomers under low energy visible light. Metalloporphyrin (*e.g.* zinc porphyrin), a highly efficient photocatalyst for photoinduced electron/energy transfer–reversible addition–fragmentation chain transfer (PET-RAFT) polymerization, was conjugated to the supports by effortless chemical grafting approaches. By virtue of the elasticity and robustness of cellulose monoliths, separation and recovery of the catalyst was accomplished through simply squeezing and washing with negligible catalyst leaching. The recyclability of the immobilized catalyst was comprehensively assessed, suggesting that catalytic performance had been sustained in the first three cycles. It is interesting to note that the catalytic activity of the composites after three cycles decreased due to demetallation of the zinc porphyrin during polymerization. Nevertheless, using free-base porphyrin with added co-catalyst (tertiary amine as a sacrificial agent) could prevent metal contamination of the final polymer products.

Published on 31 October 2017. Downloaded by UNSW Library on 12/12/2017 06:06:27.

Introduction

As an important structural component of green plants, cellulose is the most abundant organic polymer in Nature. It is considered a nearly inexhaustible source of raw materials for the continuously increasing demand for renewable and biocompatible products.[1] Formed by repetitive D-glucose building blocks, cellulose possesses many superior properties including hydrophilicity, biodegradability, chirality and a versatile semi-crystalline fibre morphology. In the form of wood, cotton and other plant fibres, cellulose is widely used as an energy source, building material and clothing.[2] As a chemical raw material, cellulose has been used for more than a century in a variety of industries because of its low cost, high strength, and high capacity for chemical modifications. Large numbers of cellulosic esters and ethers are produced on an industrial scale for use as coatings, optical films, foodstuffs, sorption media, pharmaceuticals and cosmetics. Owing to their excellent chemical and physical robustness, biocompatibility and chirality, recent works have studied cellulose as supporting matrices for the immobilization of nanoparticles,[3–5] proteins,[6,7] antibodies,[8] anticancer drugs[9,10] and heparin,[11,12] and also for the separation of chiral molecules.[13]

In this contribution, we envisioned the application of cellulose as a supporting material to immobilize organic compounds (*e.g.* photocatalysts) for heterogeneous catalysis of radical polymerization. Natural cotton and cellulose sponge, two forms of commercial fibrous and porous cellulose, were adopted due to their large surface area, light weight, elasticity, and chemical modifiability, as well as excellent compatibility with most organic solvents.

Metalloporphyrin as a family of pigments is ubiquitous and abundant in biological systems.[14] It is adaptable for chemical functionalization using diverse organic synthetic tools, and thus provides an extremely versatile platform for a variety of biomedical and materials applications ranging from artificial dye-sensitized solar cells to photodynamic therapy.[15–18] As a

[a]Centre for Advanced Macromolecular Design and Australian Centre for Nanomedicine, School of Chemical Engineering, University of New South Wales, Sydney 2052, Australia. E-mail: j.xu@unsw.edu.au, cboyer@unsw.edu.au
[b]School of Chemical Engineering, University of New South Wales, Sydney 2052, Australia
[c]Graduate School of Biomedical Engineering, University of New South Wales, Sydney 2052, Australia
[d]State Key Laboratory of Molecular Engineering of Polymers and Department of Macromolecular Science, Fudan University, 220 Han Dan Road, Shanghai 200433, China

†Electronic supplementary information (ESI) available: Experimental details, UV-vis spectra, NMR spectra, and GPC traces (Fig. S1–S14). See DOI: 10.1039/c7py01690e

Published on 31 October 2017. Downloaded by UNSW Library on 12/12/2017 06:06:27.

photocatalyst, zinc porphyrin has been demonstrated to be highly efficient and oxygen tolerant for photoinduced living radical polymerization of PET-RAFT technique.[19–27] It also presents an excellent selectivity in activating trithiocarbonates to generate radicals and subsequently control living radical polymerization.[20] However, the photocatalyst has always imparted intense colour to the final polymer products. General separation approaches include precipitation, column chromatography, and immobilization of the catalyst in organic or inorganic supports. Immobilization of the catalyst not only avoids catalyst contamination of the final product, but also affords recyclability of the catalyst.

In controlled radical polymerization, atom transfer radical polymerization (ATRP)[28–35] has been comprehensively investigated in terms of catalyst recovery due to the transition-metal complex commonly used.[36,37] Different strategies are employed for ATRP catalyst immobilization, including physical absorption,[38–40] covalent immobilization,[37,40,41] and reversible hydrogen-bonding attachment.[42] Sawamoto and co-workers prepared a phosphine ligand coordinating with ruthenium on the poly(ethylene oxide) chain to mediate polymerization in a suspension using the thermal sensitivity of poly(ethylene oxide).[43] Recently, Johnson and co-workers designed an organo/hydro-gel of poly(*N*-isopropylacrylamide) carrying a photocatalyst, 10-phenylphenothiazine, in the matrix to control polymerization through the ATRP or RAFT process mediated by both light and temperature.[44] Although the polymer hydrogel possessed acceptable strength for processing, extensive washing between cycles was required for the recycling of the catalyst loaded hydrogel.[44]

In this work, zinc porphyrin is covalently conjugated to the surface of fibrous and porous cellulose through ester bonds. This material is used as a flexible and versatile catalyst composite for the PET-RAFT polymerization of various monomers. The monoliths of cotton and cellulose sponge with excellent elasticity provide extraordinary ease of catalyst recyclability by simply squeezing and washing. Therefore, this study provides an elegant example for the demonstration of a green approach for catalyst immobilization and recycling, which has the potential for continuous commercial chemical processes and to generate interest in polymer manufacturing and design.

Results and discussion

Metalloporphyrin with the main structure of zinc tetraphenylporphyrin (ZnTPP) was employed and conjugated to fibrous and porous cellulose materials. The stepwise preparation included the functionalization of the porphyrin and subsequent bonding to the material, as illustrated in Scheme 1. Specifically, monohydroxyl functionalized tetraphenylporphyrin (TPP-OH) was first prepared using a one-step typical porphyrin synthesis[45,46] by mixing pyrrole, 4-hydroxyl benzaldehyde and benzaldehyde in the presence of propionic acid at 140 °C overnight, as reported in our previous publication.[47] After purification by column chromatography, the phenolic alcohol in TPP-OH was extended to a primary alcohol (TPP-C_2-OH) through the nucleophilic substitution reaction with 2-bromoethanol under basic conditions in order to improve the chemical stability of the ester bond after reaction with succinic anhydride to generate TPP-C_4-COOH with the primary carboxylic acid functionality. The chemical structures of TPP-C_2-OH and TPP-C_4-COOH were confirmed by ^{1}H and ^{13}C NMR (ESI, Fig. S1–S4†).

Prior to the metalation of porphyrin using zinc acetate, TPP-C_4-COOH was conjugated to cotton or sponge first *via*

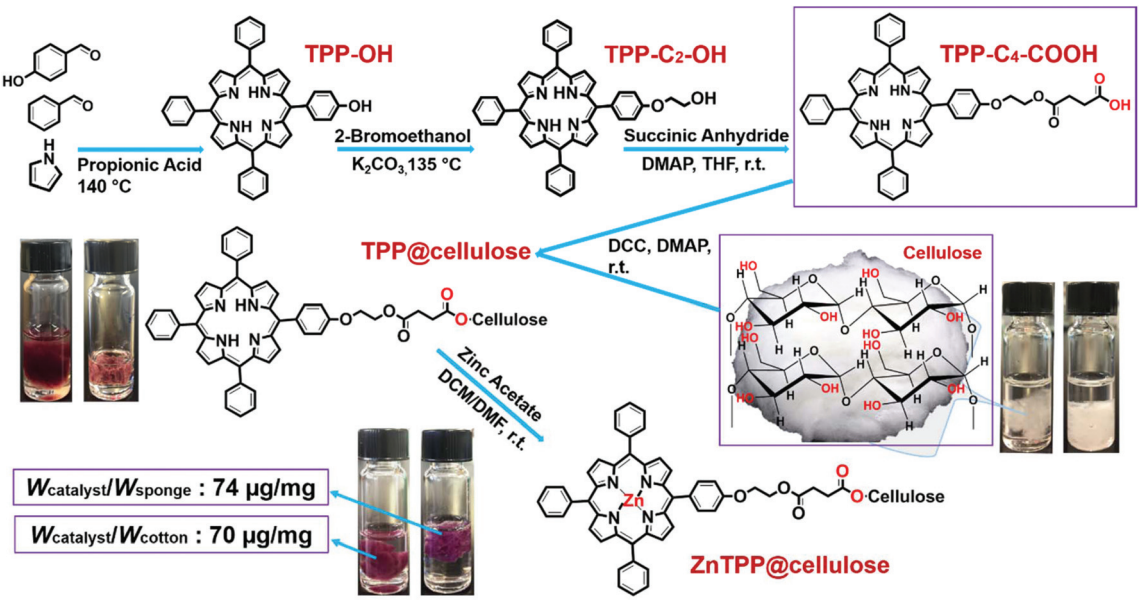

Scheme 1 Preparation of catalyst (ZnTPP) immobilized on cellulose materials, cotton and sponge.

 This journal is © The Royal Society of Chemistry 2017

Published on 31 October 2017. Downloaded by UNSW Library on 12/12/2017 06:06:27.

DCC coupling of carboxylic acid with the hydroxyl groups present in cellulose. Prior to conjugation, the cotton and sponge were cut into shape (around 20 mg) to fit the cylindrical glass vial, which was to be used as a reactor in our study. This was followed by soaking and washing with organic solvents to remove the fine particles and possible contaminants introduced during the manufacturing process. The solvents were dimethyl sulfoxide (DMSO), *N,N′*-dimethylformamide (DMF) and dichloromethane (DCM), in which subsequent organic reactions and polymerizations were performed. After washing and drying, the cotton and sponge monoliths were submerged in a DCM solution containing TPP-C_4-COOH, *N,N′*-dicyclohexyl carbodiimide (DCC), and 4-(dimethylamino)pyridine (DMAP). After three days, the elastic materials were taken out by squeezing and washing in DMSO to remove DCM and excess unreacted reagents, including the unconjugated catalyst, DCC, DMAP and the by-product dicyclohexylurea (DCU). Upon conjugation of the catalyst, the white cotton and sponge became red in colour (Scheme 1), forming the catalyst composite, TPP@cellulose. Metalation of TPP@cellulose was then conducted by immersing the composites in a DCM/DMF (1/1, v/v) mixed solution containing zinc acetate for 6 h with gentle stirring to yield ZnTPP@cellulose, after which a significant colour change from red to purple (Scheme 1) was observed. The composites were soaked in DMSO and methanol (MeOH) for two days, with the solvent changed twice to completely remove any metal contaminants and physically absorbed catalyst. To assess their structural stability against organic solvents, we immersed the composites in different solvents, which included DCM, DMSO, MeOH, chloroform and DMF. After two days of soaking, all of the tested solvents remained colourless, suggesting that the composites were intact with negligible catalyst (ZnTPP) leaching (ESI, Fig. S5†).

Most importantly, despite frequent physical squeezing and chemical soaking, the whole process of catalyst immobilization did not destroy fibrous and porous microstructures of the materials, showing its robustness, which was visualized by scanning electron microscopy (SEM) (Fig. 1). The catalyst loading was found by inductively coupled plasma optical emission spectroscopy (ICP-OES) to be 70 μg mg^{-1} and 74 μg mg^{-1} ($W_{catalyst}/W_{composite}$, weight percentage of the catalyst on the composite) for ZnTPP@cotton and ZnTPP@sponge, respectively.

Subsequently, to assess the catalytic efficiency of the immobilized photoredox catalyst on the composites, these two materials were employed as heterogeneous catalysts for PET-RAFT polymerizations of methyl acrylate (MA) using 2-cyano-2-propyl dodecyl trithiocarbonate (CPDTC, Scheme 2) as a RAFT agent in DMSO under red LED light (λ_{max} = 635 nm, 0.2 mW cm^{-2}). The molar ratio of [MA] : [CPDTC] = 200 : 1 was applied for both polymerizations catalysed by ZnTPP@cotton and ZnTPP@sponge. One piece of cotton or sponge (20 mg) containing 1.4–1.5 mg ZnTPP was immersed in the reaction mixture of monomer (MA, 0.5 mL), RAFT agent (CPDTC, 9.5 mg) and solvent (DMSO, 0.5 mL). The liquid fully occupied the free space of the cotton or sponge pieces. After nitrogen degassing, the sealed reaction vessel was placed under red light. Small aliquots of the solution were withdrawn at predetermined intervals for the measurement of monomer conversions by ^{1}H NMR and number-average molecular weights (M_n) and polydispersities (M_w/M_n) by gel permeation chromatography (GPC), which provided details of the kinetics profile (Fig. 2).

After 24 h reaction, the monomer conversions of ZnTPP@cotton and ZnTPP@sponge catalysed polymerizations of MA were 72% and 70%, respectively. The control experi-

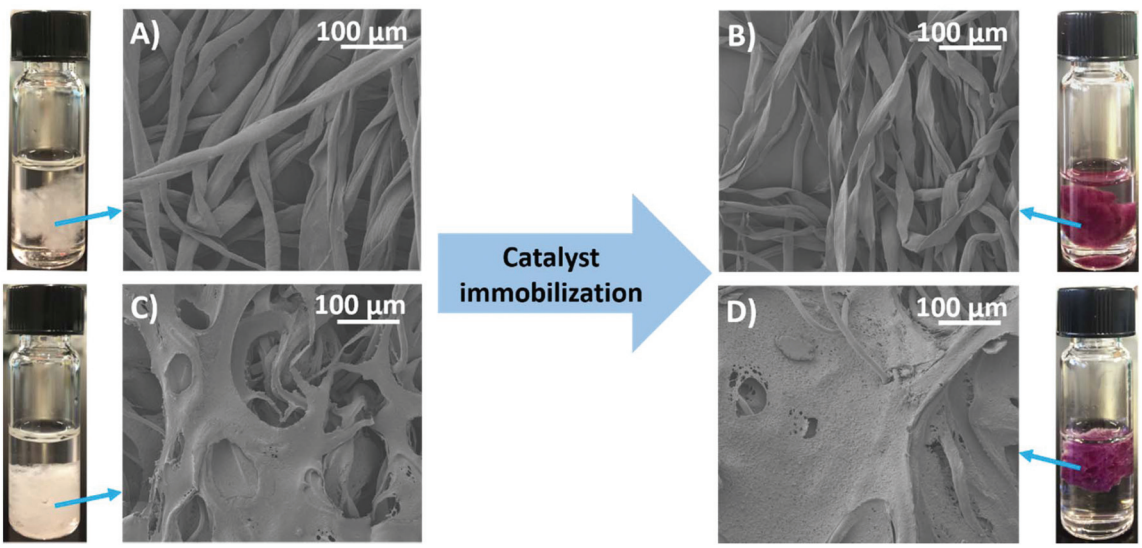

Fig. 1 SEM images of the (A) original cotton, (B) ZnTPP@cotton composite, (C) original sponge, and (D) ZnTPP@sponge composite and the corresponding optical images of materials soaked in DMSO on the sides.

Published on 31 October 2017. Downloaded by UNSW Library on 12/12/2017 06:06:27.

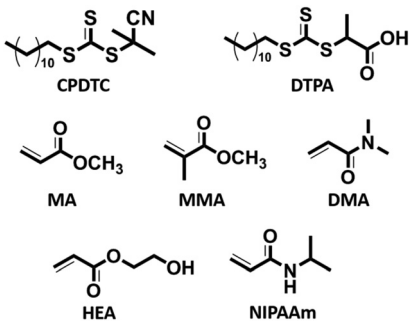

Scheme 2 The monomers and RAFT agent investigated in this study. CPDTC: 2-cyano-2-propyl dodecyl trithiocarbonate; DTPA: 2-(dodecylthiocarbonothioylthio) propionic acid; MA: methyl acrylate; MMA: methyl methacrylate; HEA: 2-hydroxyethyl acrylate; DMA: *N,N′*-dimethylacrylamide; NIPAAm: *N*-isopropylacrylamide.

ments in the absence of light or catalyst composites resulted in negligible monomer conversion. A linear plot of $\ln([M]_0/[M]_t)$ against exposure time was obtained in both ZnTPP@cotton (Fig. 2A) and ZnTPP@sponge (Fig. 2B) mediated polymerization, suggesting constant concentrations of the propagating radicals throughout the polymerization. Interestingly, the apparent propagating rate constants (k_p^{app}) derived from the slope of the plotted curves suggested comparable values (5.35×10^{-2} h^{-1} for ZnTPP@cotton and 5.70×10^{-2} h^{-1} ZnTPP@sponge), which matched well with the almost equivalent catalyst concentrations in both composite materials (70 μg mg^{-1} *vs.* 74 μg mg^{-1}). As expected, the polymerization rate in a heterogeneous system using an immobilized catalyst was much slower than that under homogeneous conditions using free ZnTPP (k_p^{app}(red) = 1.3×10^{-2} min^{-1} (equal to 7.8×10^{-1} h^{-1})),[20] owing to the greatly reduced heterogeneous efficiency, limited access of the RAFT agent to the catalyst on the surface and decreased light penetration in the presence of fibrous and porous materials. SEM images (Fig. 1A and C) of the materials reveal the presence of more than 50 μm-sized fibres and macro-pores, suggesting that the surface area was not high enough compared with homogeneous or nano-sized heterogeneous systems. It is worth noting that an inhibition period (around 3 h) was observed in a ZnTPP@sponge catalysed reaction (Fig. 2B), which was hypothesized to be attributed to trapped oxygen in the small pores of the sponge. The sponge possesses a broadly distributed pore size ranging from 1 to 1000 μm (Fig. 1C and D) and the air accommodated in these small pores was not completely removed by the general deoxygenation procedure (nitrogen bubbling). On the other hand, cotton is a fibrous material with a relatively uniform fibre size and no space to retain air after the deoxygenation process (Fig. 1A and B).

Well controlled polymerizations were observed with a linear increase of the number-average molecular weight (M_n) *versus* monomer conversion, with good agreement with the theoretical values in addition to low polydispersities (Fig. 2C for ZnTPP@cotton and Fig. 2D for ZnTPP@sponge), showcasing the living features of the polymerization. Furthermore, molecular weight distributions showed a clear shift from low to high molecular weights during the polymerization (Fig. 2E for ZnTPP@cotton and Fig. 2F for ZnTPP@sponge). In addition, this process was able to temporally control the polymerization by switching the light ON and OFF as expected (ESI, Fig. S6†). Moreover, to confirm the living character of this polymerization and the integrity of the end-group, chain-extensions with *N,N′*-dimethylacrylamide (DMA) were performed. A PMA macroRAFT agent ($M_{n,GPC\text{-}cotton}$ = 8300 g mol^{-1}, M_w/M_n = 1.12, and 48% monomer conversion) was prepared by PET-RAFT

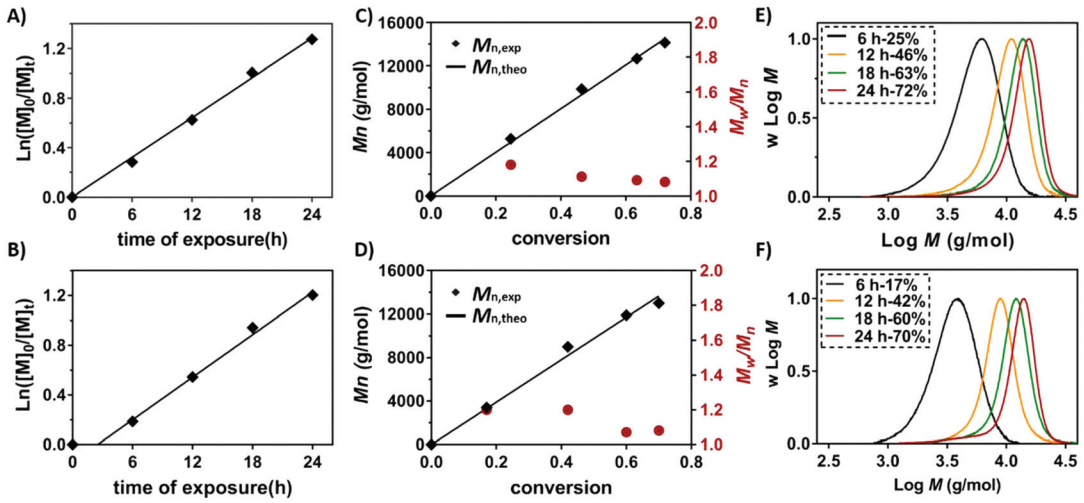

Fig. 2 Kinetics study of the PET-RAFT polymerization of MA with CPDTC as the chain transfer agent and immobilized catalyst under red light irradiation (λ_{max} = 635 nm, 0.2 mW cm^{-2}), using a molar ratio of [MA]/[CPDTC] = 200 : 1 in DMSO. The dependence of $\ln([M]_0/[M]_t)$ on exposure time in the polymerization catalysed by ZnTPP@cotton (A) and ZnTPP@sponge (B); evolution of M_n *versus* the monomer conversion in the polymerization catalysed by ZnTPP@cotton (C) and ZnTPP@sponge (D); molecular weight distributions after exposure to red light for different periods of time in the polymerization catalysed by ZnTPP@cotton (E) and ZnTPP@sponge (F).

 This journal is © The Royal Society of Chemistry 2017

Published on 31 October 2017. Downloaded by UNSW Library on 12/12/2017 06:06:27.

polymerization catalysed by ZnTPP@cotton under red light irradiation in DMSO. After purification of the macroRAFT agent through direct precipitation, PMA-*b*-PDMA diblock copolymers with narrow molecular weight distributions ($M_{n,GPC\text{-}cotton}$ = 24 500 g mol^{-1}, M_w/M_n = 1.10, and 51% monomer conversion) were obtained through chain extension of the macroRAFT agent under red light irradiation, which was indicated by a clear shift of the peak of the PMA macroRAFT agent in the absence of a tailing or macroRAFT residue (ESI, Fig. S7†).

The great benefit of the use of the immobilized catalyst in fibrous and porous composites for polymerization is the facile separation of the photoredox catalyst from the reaction solution by simply squeezing and washing the elastic materials. However, with such a process, there is a concern of catalyst leaching from the support during the period of usage, which may be realized through the cleavage of the ester bonds between the ZnTPP moieties and cellulose. Therefore, catalyst contamination in the reaction solution leached from the composite during polymerization is an important indicator to assess the viability of this strategy. After separation of the material from the reaction solution, the liquid in the vial was light yellow (ESI, Fig. S8B and C†), showing no difference to the reaction media prior to polymerization, suggesting minimal catalyst leaching during the reaction, whilst in homogeneous PET-RAFT polymerizations mediated by ZnTPP, the colour of the reaction mixture containing 80 ppm catalyst (relative to monomer concentration) was intensely purple after polymerization (ESI, Fig. S8A†). UV-Vis analysis was performed for the reaction mixture to quantify the free catalyst leached from the ZnTPP@cellulose composite during the polymerization. The UV-Vis spectra (ESI, Fig. S10†) revealed very tiny peaks at 428 nm, assigned to the maximum Q-band absorption of ZnTPP moieties present on the ZnTPP@cotton and ZnTPP@sponge. It was noted that the absorption of the RAFT agent (trithiocarbonate) also peaks in this area, which complicates accurate measurement of the leached catalyst. Nevertheless, the estimation was conducted from UV-Vis data using an established ZnTPP standard (ESI, Fig. S9†). The amount of the free catalyst (ZnTPP derivatives) in the reaction mixture after polymerization was calculated to be a maximum of 0.49 μg ZnTPP (equivalent to 0.35 wt‰ of the original loading) in the reaction solution (ESI, Fig. S10†), which is negligible. Meanwhile, to evaluate the contribution of the leached catalyst (0.49 μg) to the polymerization, we performed a control experiment of MA polymerization by PET-RAFT technique under identical conditions using 2 μg (4 times the amount of the leached catalyst) ZnTPP as a photoredox catalyst instead of the cotton or sponge composite. Results showed no monomer conversion (~0%) after 24 h polymerization, suggesting that polymerization of MA was contributed completely by the immobilized catalyst on the cellulose material rather than the free catalyst leached from the composite.

To demonstrate the versatility and robustness of the catalyst immobilized on porous fibrous materials for heterogeneously catalysing controlled radical polymerization, various functional monomers (Scheme 2), including 2-hydroxylethyl acrylate (HEA), DMA, *N*-isopropylacrylamide (NIPAAm), and methyl methacrylate (MMA), were investigated. In addition, another RAFT agent, 2-(dodecylthiocarbonothioylthio)propionic acid (DTPA), was also tested to assess the stability of the immobilized catalyst against carboxylic acid residues. ZnTPP@cotton was used in these polymerizations under identical conditions to those for MA polymerization. Comparable conversions were observed on these monomers over a certain period of polymerization time (11–24 h for acrylamides and acrylates and 39 h for MMA). The results for MA, DMA and NIPAAM (no. 1, 4 and 5, Table 1) with CPDTC and for MA with DTPA (no. 6, Table 1) demonstrated excellent control over the molecular weights and polydispersities (M_w/M_n < 1.15; GPC curves shown in the ESI, Fig. S11†). The polymerization of MMA revealed the highest polydispersity (M_w/M_n = 1.26), which was attributed to the trithiocarbonate generally displaying a low chain transfer constant to control methacrylate polymerization. In the case of HEA, a relatively high polydispersity (M_w/M_n = 1.24) and a high molecular weight shoulder in the GPC curve (ESI, Fig. S11†) were always obtained at high monomer conversion (62%) and monomer concentration (3.17 M), due to the presence of the difunctional crosslinker generated from *trans*-esterification.[48,49]

UV-Vis analysis was also conducted to analyse the amount of free catalyst leached from the composites into the reaction solution during polymerization (ESI, Fig. S12†). In the polymerization of HEA after 11 h light irradiation, a much larger amount of free catalyst (3.3 μg ZnTPP/20 mg ZnTPP@cotton) was detected than those of other monomers

Table 1 PET-RAFT Polymerization of different monomers using ZnTPP@cotton with different trithiocarbonate compounds

No.	Exp. cond.[a] [M] : [RAFT]	RAFT	Monomer	Time (h)	α^b (%)	$M_{n,exp}{}^c$ (GPC) (g mol^{-1})	PDI[c]
1	200 : 1	CPDTC	MA	24	72	14 100	1.08
2	200 : 1	CPDTC	MMA	39	74	13 600	1.26
3	200 : 1	CPDTC	HEA	11	62	27 100	1.24
4	200 : 1	CPDTC	DMA	24	63	10 600	1.11
5	200 : 1	CPDTC	NIPAAM	24	62	24 300	1.13
6	200 : 1	DTPA	MA	24	40	6000	1.11

[a] The reactions were performed at room temperature under red light irradiation (λ_{max} = 635 nm, 0.2 mW cm^{-2}) using 20 mg ZnTPP@cotton. [b] Monomer conversion was determined by ^{1}H NMR spectroscopy. [c] Molecular weight and polydispersity were determined by GPC (DMAc was used as an eluent) calibrated with a poly(methyl methacrylate) (PMMA) standard for the synthesized polymers.

Published on 31 October 2017. Downloaded by UNSW Library on 12/12/2017 06:06:27.

(~0.49 μg ZnTPP/20 mg ZnTPP@cotton), which was attributed to the possible hydrolysis of the ester bond or *trans*-esterification with the hydroxyl functionality of HEA. The amount of catalyst leached during the polymerization of HEA was still considered to be negligible compared to the total amount of the catalyst conjugated to the cellulose support (1400 μg ZnTPP/20 mg ZnTPP@cotton, ~2 wt‰).

Recyclability of the immobilized catalyst is an equally important parameter, which was evaluated *via* measuring the monomer conversions throughout the repetitive cycles of PET-RAFT polymerization of MA using the same piece of catalyst composite under identical conditions. After each reaction cycle, catalyst@cellulose was separated from the reaction mixture, washed with DMSO, and then soaked in DMSO overnight prior to the next reaction cycle. Interestingly, although the amount of the immobilized catalyst was comparable for cotton and sponge composites, the system of ZnTPP@cotton showed superior catalytic performance (~5% higher monomer conversions in each reaction cycle) than that of ZnTPP@sponge, regardless of the number of recycles (Fig. 3A). This could be explained by two reasons: (1) the sponge system always has an induction period (~3 h) as suggested in Fig. 2, which causes lower monomer conversion at the same length of reaction; (2) fibrous cotton possesses a uniform morphology and a high flexibility when immersed in DMSO, whereas sponge was relatively rigid and less uniform in morphology, decreasing light penetration.

Moreover, Fig. 3A clearly showed that the repeated use of both ZnTPP@cotton and ZnTPP@sponge in the first three cycles did not impair the catalytic efficiency with comparable monomer conversions (65%, 67% and 59% for ZnTPP@cotton and 59%, 51% and 55% for ZnTPP@sponge) after 24 h polymerization. However, the monomer conversions unfortunately dropped after three cycles, giving the values of 48% and 36% for ZnTPP@cotton and 39% and 28% for ZnTPP@sponge for the fourth and fifth cycles, respectively. As demonstrated by UV-Vis analysis of the reaction mixtures, there was negligible (<2 wt‰) ZnTPP catalyst leached out from both composites of sponge and cotton, regardless of the numbers of recycles (ESI, Fig. S10A†). Thus, it is surprising to observe a significant decrease of catalytic activity after three cycles. This result motivated us to explore the possible reasons.

The demetallation of zinc is most likely the possible reason for the reduced catalytic activity. Indeed, the demetallation behaviour of metal porphyrin or chlorin is quite common under specific conditions, which result in the production of free-base tetraphenylporphyrin (TPP).[50–52] In our previous report, we found that TPP without zinc metal in the centre is not an efficient catalyst for trithiocarbonate activation to mediate PET-RAFT polymerization of acrylates.[47] In order to prove our hypothesis, ICP-OES analysis of the reaction mixture after polymerization was conducted to monitor the amount of zinc element leached from the composites. Fig. 3B showed that the zinc amount in the initial ZnTPP@cotton composite (20 mg) was 109 μg before polymerization. After the first cycle of polymerization, the reaction mixture contained 36 μg zinc (33 wt% of the total zinc amount), whereas the reaction mixture before polymerization was almost zero. In other words, 36 μg zinc (33 wt%) leached out from the composite during the first use of the composite for polymerization. After the second cycle, 31 μg zinc (28 wt% of the total zinc amount) was detected in the second reaction mixture. Although only 42 μg zinc (39 wt% of the total zinc amount) was left on the composite after two cycles, the molar amount of effective catalyst in the third polymerization cycle was 116 ppm relative to the monomer, which was efficient in catalysing the reaction. In our previous report, increasing the catalyst concentration over 50 ppm did not promote the polymerization rates due to undesirable self-quenching of ZnTPP, which may include coupling of excitons and excimer formation. Therefore, in the first three cycles, the catalyst concentrations are more than 50 ppm, giving similar reaction rates.[20]

After the third cycle, the final composite was analysed by ICP-OES after washing and drying and only 10 μg zinc (9 wt%

A)

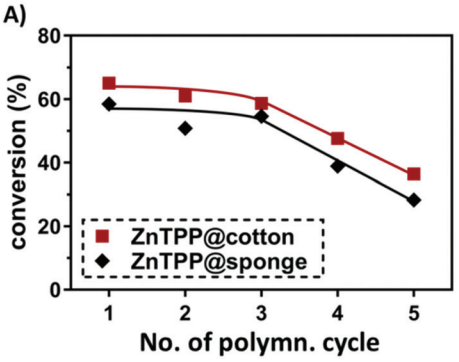

B)

Reaction mixture: 1 g	ZnTPP@cotton: 20 mg			
	Before polymn	After polymn		
		1st	2nd	3rd
Zn amnt in reaction mixture (μg)	0	36[a]	31[a]	32[b]
Zn amnt in ZnTPP@cotton (μg)	109[a]	73[b]	42[b]	10[a]

Fig. 3 (A) Monomer conversions of PET-RAFT polymerization of MA after 24 h reaction using CPDTC as the chain transfer agent mediated by ZnTPP@cotton and ZnTPP@sponge under red light irradiation in different polymerization cycles; (B) The Zn amount in ZnTPP@cotton and the reaction mixture before polymerization and after the 1st, 2nd, and 3rd reaction cycles of the polymerization of MA using CPDTC as a chain transfer agent under red light irradiation. [a] Data were collected from ICP-OES analysis, [b] data were calculated by using: 73 = (109 – 36); 42 = (73 – 31); 32 = (42 – 10).

 This journal is © The Royal Society of Chemistry 2017

Published on 31 October 2017. Downloaded by UNSW Library on 12/12/2017 06:06:27.

of the total zinc amount, 25 ppm catalyst relative to monomer) was left. These results showed that around 30 wt% of the immobilized catalyst (ZnTPP) on the composite lost their zinc centres after each cycle of polymerization. A possible explanation could be the complexation (moderate S–Zn bond) between the thiocarbonylthio moiety in the RAFT agent and zinc. During the reaction, the porphyrin ring was anchored on the fibrous and porous materials, whilst zinc was dragged by the RAFT agent and propagating polymer chains, thereby zinc was dissociated from the immobilized catalyst. Since the zinc centre is vital for catalytic efficiency, we observed decreased catalytic activities upon the continuous demetallation of zinc porphyrin in the catalyst composite. Regarding the kinetics study (Fig. 2) in the first cycle of polymerization, 33% of demetallation of zinc porphyrin does not affect polymerization behaviour. Fortunately, despite the decrease in catalytic efficiency, the synthesized polymers in all the reaction cycles showed good control over molecular weight distributions (ESI, Fig. S13†).

To address the metal contamination in the polymer product, an effective approach is by using TPP@cellulose with free-base porphyrin conjugated to the cellulose as the photocatalyst for PET-RAFT polymerization. However, a sacrificial agent (*e.g.* triethylamine, TEA) has to be introduced to play the role of a co-catalyst, through electron donation to the excited porphyrin and then to the RAFT agent to generate the desired carbon-centred radicals. The molar ratio of [MA] : [DTPA] : [TEA] = 200 : 1 : 1 was used for the polymerization in the presence of TPP@cotton (20 mg) in DMSO under red light irradiation. A monomer conversion of 79% was obtained after 21 h reaction, accompanied by good control over the molecular weight and the molecular weight distribution (ESI, Fig. S14A†). Negligible catalyst leaching from the composite was concluded from the UV-Vis spectrum of the reaction mixture after polymerization, showing a very small peak at 428 nm (the maximum absorption of TPP) on the bump of trithiocarbonate absorption.

Conclusions

In summary, metalloporphyrin, a photoredox catalyst, was successfully modified and conjugated to fibrous and porous cellulose materials. These immobilized catalysts were able to mediate PET-RAFT polymerization with good control over the molecular weights and molecular weight distributions. The versatility of the immobilized catalyst was confirmed by the polymerization of different functional monomers. More importantly, they can be easily recovered from the reaction mixture after polymerization and reused for three cycles without sacrificing the catalytic activity, despite the continuous demetallation of zinc porphyrin during polymerization. This catalyst immobilization strategy is facile and green due to the abundant and sustainable sources of cellulose materials, and is widely applicable to other functionalized catalysts and hydroxyl group-abundant supports with diverse potential applications.

Conflicts of interest

There are no conflicts to declare.

Acknowledgements

J. X. and C. B. would like to acknowledge the Australian Research Council (ARC) for their Future Fellowships (FT160100095 and FT12010096).

Notes and references

1 D. Klemm, B. Heublein, H.-P. Fink and A. Bohn, *Angew. Chem., Int. Ed.*, 2005, **44**, 3358–3393.
2 N. Grishkewich, N. Mohammed, J. Tang and K. C. Tam, *Curr. Opin. Colloid Interface Sci.*, 2017, **29**, 32–45.
3 Y. Li, L. Xu, B. Xu, Z. Mao, H. Xu, Y. Zhong, L. Zhang, B. Wang and X. Sui, *ACS Appl. Mater. Interfaces*, 2017, **9**, 17155–17162.
4 J. Van Rie and W. Thielemans, *Nanoscale*, 2017, **9**, 8525–8554.
5 X. Wu, Z. Shi, S. Fu, J. Chen, R. M. Berry and K. C. Tam, *ACS Sustainable Chem. Eng.*, 2016, **4**, 5929–5935.
6 C. Kauffmann, O. Shoseyov, E. Shpigel, E. A. Bayer, R. Lamed, Y. Shoham and R. T. Mandelbaum, *Environ. Sci. Technol.*, 2000, **34**, 1292–1296.
7 Y. Zhang and O. J. Rojas, *Biomacromolecules*, 2017, **18**, 526–534.
8 V. S. Raghuwanshi, J. Su, C. J. Garvey, S. A. Holt, P. J. Holden, W. J. Batchelor and G. Garnier, *Biomacromolecules*, 2017, **18**, 2439–2445.
9 E. Anaya-Plaza, E. van de Winckel, J. Mikkilä, J.-M. Malho, O. Ikkala, O. Gulías, R. Bresolí-Obach, M. Agut, S. Nonell, T. Torres, M. A. Kostiainen and A. de la Escosura, *Chem. – Eur. J.*, 2017, **23**, 4320–4326.
10 B. Fejerskov, M. T. Jarlstad Olesen and A. N. Zelikin, *Adv. Drug Delivery Rev.*, 2017, DOI: 10.1016/j.addr.2017.04.013.
11 F. Zia, K. M. Zia, M. Zuber, S. Tabasum and S. Rehman, *Int. J. Biol. Macromol.*, 2016, **84**, 101–111.
12 L. Hou, W. M. R. N. Udangawa, A. Pochiraju, W. Dong, Y. Zheng, R. J. Linhardt and T. J. Simmons, *ACS Biomater. Sci. Eng.*, 2016, **2**, 1905–1913.
13 L. Nováková and M. Douša, *Anal. Chim. Acta*, 2017, **950**, 199–210.
14 M. Patel and B. J. Day, *Trends Pharmacol. Sci.*, 1999, **20**, 359–364.
15 K. S. Suslick, N. A. Rakow, M. E. Kosal and J.-H. Chou, *J. Porphyrins Phthalocyanines*, 2000, **04**, 407–413.
16 W.-Y. Gao, C.-Y. Tsai, L. Wojtas, T. Thiounn, C.-C. Lin and S. Ma, *Inorg. Chem.*, 2016, **55**, 7291–7294.

Published on 31 October 2017. Downloaded by UNSW Library on 12/12/2017 06:06:27.

17 A. Maurin and M. Robert, *J. Am. Chem. Soc.*, 2016, **138**, 2492–2495.
18 X.-L. Lv, K. Wang, B. Wang, J. Su, X. Zou, Y. Xie, J.-R. Li and H.-C. Zhou, *J. Am. Chem. Soc.*, 2017, **139**, 211–217.
19 J. Xu, K. Jung, A. Atme, S. Shanmugam and C. Boyer, *J. Am. Chem. Soc.*, 2014, **136**, 5508–5519.
20 S. Shanmugam, J. Xu and C. Boyer, *J. Am. Chem. Soc.*, 2015, **137**, 9174–9185.
21 J. Xu, S. Shanmugam, C. Fu, K.-F. Aguey-Zinsou and C. Boyer, *J. Am. Chem. Soc.*, 2016, **138**, 3094–3106.
22 J. Xu, C. Fu, S. Shanmugam, C. J. Hawker, G. Moad and C. Boyer, *Angew. Chem., Int. Ed.*, 2017, **56**, 8376–8383.
23 N. Corrigan, S. Shanmugam, J. Xu and C. Boyer, *Chem. Soc. Rev.*, 2016, **45**, 6165–6212.
24 N. Corrigan, D. Rosli, J. W. J. Jones, J. Xu and C. Boyer, *Macromolecules*, 2016, **49**, 6779–6789.
25 J. Yeow, R. Chapman, J. Xu and C. Boyer, *Polym. Chem.*, 2017, **8**, 5012–5022.
26 S. Dadashi-Silab, S. Doran and Y. Yagci, *Chem. Rev.*, 2016, **116**, 10212–10275.
27 M. R. Hill, R. N. Carmean and B. S. Sumerlin, *Macromolecules*, 2015, **48**, 5459–5469.
28 K. Matyjaszewski, *Macromolecules*, 2012, **45**, 4015–4039.
29 E. Blasco, M. B. Sims, A. S. Goldmann, B. S. Sumerlin and C. Barner-Kowollik, *Macromolecules*, 2017, **50**, 5215–5252.
30 R. B. Grubbs and R. H. Grubbs, *Macromolecules*, 2017, **50**, 6979–6997.
31 J. C. Theriot, C.-H. Lim, H. Yang, M. D. Ryan, C. B. Musgrave and G. M. Miyake, *Science*, 2016, **352**, 1082–1086.
32 N. J. Treat, H. Sprafke, J. W. Kramer, P. G. Clark, B. E. Barton, J. Read de Alaniz, B. P. Fors and C. J. Hawker, *J. Am. Chem. Soc.*, 2014, **136**, 16096–16101.
33 X. Pan, C. Fang, M. Fantin, N. Malhotra, W. Y. So, L. A. Peteanu, A. A. Isse, A. Gennaro, P. Liu and K. Matyjaszewski, *J. Am. Chem. Soc.*, 2016, **138**, 2411–2425.
34 M. Ciftci, G. Yilmaz and Y. Yagci, *J. Photopolym. Sci. Technol.*, 2017, **30**, 385–392.
35 Z. Huang, Y. Gu, X. Liu, L. Zhang, Z. Cheng and X. Zhu, *Macromol. Rapid Commun.*, 2017, **38**, 1600461.
36 M. Ding, X. Jiang, L. Zhang, Z. Cheng and X. Zhu, *Macromol. Rapid Commun.*, 2015, **36**, 1702–1721.
37 G. Kickelbick, H.-J. Paik and K. Matyjaszewski, *Macromolecules*, 1999, **32**, 2941–2947.
38 S. Barrientos-Ramírez, G. M. D. Oca-Ramírez, E. V. Ramos-Fernández, A. Sepúlveda-Escribano, M. M. Pastor-Blas and A. González-Montiel, *Appl. Catal., A*, 2011, **406**, 22–33.
39 D. M. Haddleton, D. J. Duncalf, D. Kukulj and A. P. Radigue, *Macromolecules*, 1999, **32**, 4769–4775.
40 X. Jiang, J. Wu, L. Zhang, Z. Cheng and X. Zhu, *Macromol. Rapid Commun.*, 2016, **37**, 143–148.
41 E. Duquesne, P. Degee, J. Habimana and P. Dubois, *Chem. Commun.*, 2004, 640–641, DOI: 10.1039/B316645G.
42 J. Yang, S. Ding, M. Radosz and Y. Shen, *Macromolecules*, 2004, **37**, 1728–1734.
43 T. Yoshitani, Y. Watanabe, T. Ando, M. Kamigaito and M. Sawamoto, in *Controlled/Living Radical Polymerization*, American Chemical Society, 2006, vol. 944, ch. 2, pp. 14–25.
44 M. Chen, S. Deng, Y. Gu, J. Lin, M. J. MacLeod and J. A. Johnson, *J. Am. Chem. Soc.*, 2017, **139**, 2257–2266.
45 L. Xu, L. Liu, F. Liu, H. Cai and W. Zhang, *Polym. Chem.*, 2015, **6**, 2945–2954.
46 F. D'Souza, G. R. Deviprasad, M. E. El-Khouly, M. Fujitsuka and O. Ito, *J. Am. Chem. Soc.*, 2001, **123**, 5277–5284.
47 J. Xu, S. Shanmugam and C. Boyer, *ACS Macro Lett.*, 2015, **4**, 926–932.
48 K. L. Robinson, M. A. Khan, M. V. de Paz Báñez, X. S. Wang and S. P. Armes, *Macromolecules*, 2001, **34**, 3155–3158.
49 K. Bian and M. F. Cunningham, *Macromolecules*, 2005, **38**, 695–701.
50 Y. Saga, S. Hojo and Y. Hirai, *Bioorg. Med. Chem.*, 2010, **18**, 5697–5700.
51 F. Li, S. Gentemann, W. A. Kalsbeck, J. Seth, J. S. Lindsey, D. Holten and D. F. Bocian, *J. Mater. Chem.*, 1997, **7**, 1245–1262.
52 N. K. Giri, A. Banerjee, R. W. J. Scott, M. F. Paige and R. P. Steer, *Phys. Chem. Chem. Phys.*, 2014, **16**, 26252–26260.

 This journal is © The Royal Society of Chemistry 2017